

Critical role of peroxisome proliferator-activated receptor α in promoting platelet hyperreactivity and thrombosis under hyperlipidemia

Li Li,^{1,2*} Jiawei Zhou,^{3*} Shuai Wang,^{1,2*} Lei Jiang,⁴ Xiaoyan Chen,^{1,2} Yangfan Zhou,^{1,2} Jingke Li,^{1,2} Jingqi Shi,^{1,2} Pu Liu,⁵ Zheyue Shu,^{6,7} Frank J. Gonzalez,⁸ Aiming Liu^{9#} and Hu Hu^{1,2,10#}

¹Department of Pathology and Pathophysiology and Bone Marrow Transplantation Center of the First Affiliated Hospital, Zhejiang University School of Medicine, Hangzhou, China;

²Institute of Hematology, Zhejiang Engineering Laboratory for Stem Cell and Immunotherapy, Zhejiang University, Hangzhou, China; ³State Key Laboratory of Diagnosis and Treatment for Infectious Diseases, The First Affiliated Hospital, College of Medicine, Zhejiang University, Hangzhou, China; ⁴Department of Pathology, Zhejiang Provincial Key Laboratory of Pathophysiology, Ningbo University School of Medicine, Ningbo, China;

⁵Department of Pathology of the First Affiliated Hospital, Zhejiang University School of Medicine, Hangzhou, China; ⁶Division of Hepatobiliary and Pancreatic Surgery, Department of Surgery, First Affiliated Hospital, Zhejiang University School of Medicine, Hangzhou, China; ⁷Key Laboratory of Combined Multi-Organ Transplantation, Ministry of Public Health, Hangzhou, China; ⁸Laboratory of Metabolism, Center for Cancer Research, National Cancer Institute, NIH, Bethesda, MD, USA; ⁹Ningbo University School of Medicine, Ningbo, China; ¹⁰Key Laboratory of Disease Proteomics of Zhejiang Province, Hangzhou, China.

*LL, JZ and SW contributed equally as co-first authors.

#AML and HH contributed equally as co-senior authors.

Correspondence:

Hu Hu
huhu@zju.edu.cn

Aiming Liu
liuaiming@nbu.edu.cn

Received: August 5, 2021.


Accepted: September 29, 2021.

Prepublished: October 7, 2021.

<https://doi.org/10.3324/haematol.2021.279770>

©2022 Ferrata Storti Foundation

Haematologica material is published under a CC

BY-NC license 

Abstract

Platelet hyperreactivity and increased atherothrombotic risk are specifically associated with dyslipidemia. Peroxisome proliferator-activated receptor alpha (PPAR α) is an important regulator of lipid metabolism. It has been suggested to affect both thrombosis and hemostasis, yet the underlying mechanisms are not well understood. In this study, the role and mechanism of PPAR α in platelet activation and thrombosis related to dyslipidemia were examined. Employing mice with deletion of PPAR α (*Ppara*^{-/-}), we demonstrated that PPAR α is required for platelet activation and thrombus formation. The effect of PPAR α is critically dependent on platelet dense granule secretion, and is contributed by p38MAPK/Akt, fatty acid β -oxidation, and NAD(P)H oxidase pathways. Importantly, PPAR α and the associated pathways mediated a prothrombotic state induced by a high-fat diet and platelet hyperactivity provoked by oxidized low density lipoproteins. Platelet reactivity was positively correlated with the levels of expression of PPAR α , as revealed by data from wild-type, chimeric (*Ppara*^{+/-}), and *Ppara*^{-/-} mice. This positive correlation was recapitulated in platelets from hyperlipidemic patients. In a lipid-treated megakaryocytic cell line, the lipid-induced reactive oxygen species-NF- κ B pathway was revealed to upregulate platelet PPAR α in hyperlipidemia. These data suggest that platelet PPAR α critically mediates platelet activation and contributes to the prothrombotic status under hyperlipidemia.

Introduction

Underpinned by platelet hyperactivity, atherothrombotic disease is the leading cause of mortality and morbidity worldwide. Dyslipidemia has been firmly established as a risk factor for atherothrombotic disease.^{1,2} Despite the vigorous efforts that have been devoted to establishing the pathways leading to platelet hyperactivity in dyslipidemia,^{3,4} the mechanisms responsible are still unclear. Identification of key targets by which dyslipidemia regulates platelet activity is im-

perative for the prevention and management of atherothrombotic disease.

Oxidized low density lipoproteins (oxLDL), the product of dysfunctional lipid metabolism, are major promoters of a prothrombotic state in both animal models and human patients.^{5,6} Scavenger receptor CD36 and signaling pathways such as Src family kinases (SFK), mitogen-activated protein kinases and reactive oxygen species (ROS) are involved in oxLDL-induced platelet activation.⁷⁻⁹ Molecules involved in lipid metabolism such as the transcription factors farnesoid X receptor,¹⁰ liver X receptor,¹¹ and PPAR¹²⁻¹⁴

are also expressed in platelets. How these molecules interact with the established platelet activation network is ill-defined.

PPAR α is a major regulator of lipid metabolism in nucleated cells by upregulating the transcription of lipid-metabolizing enzymes, such as carnitine palmitoyl-CoA transferase-I (CPT-I) and acyl-CoA oxidase.¹⁵⁻¹⁷ It is expressed in anucleate platelets and was reported to play roles in thrombosis and hemostasis.^{18,19} Although PPAR α may interact with protein kinase C during platelet activation,¹⁸ the underlying signaling mechanism has not been elucidated. A variety of metabolic and pathological conditions are related to PPAR α expression,²⁰⁻²² but it has not been explored whether or how platelet activation is regulated by PPAR α .

In this study, we investigated the role of PPAR α in dyslipidemia-related prothrombotic potential and platelet hyperactivity. PPAR α expression in platelets was enhanced in both a hyperlipidemic mouse model and patients, which correlated well with platelet hyperactivity. The mechanism increasing PPAR α expression in platelets and the platelet functions targeted by PPAR α were explored.

Methods

Subjects

The procedures in human subjects were approved by the Ethics Committee of the First Affiliated Hospital of Zhejiang University, and informed consent was obtained from the study participants. Blood from 36 patients with hypertriglyceridemia, 16 patients with hypercholesterolemia and 31 healthy subjects was obtained. None of the participants had taken any antiplatelet or other nonsteroidal anti-inflammatory drugs for at least 14 days before blood collection.

None of the patients had clinical evidence of cardiovascular disease (according to their clinical history, physical examination, and electrocardiogram). Moreover, exclusion criteria for all subjects included renal insufficiency, proteinuria, altered hepatic function and alcohol abuse. Patients with diabetes mellitus (fasting blood glucose level >115 mg/dL or treatment with a hypoglycemic agent), hypertension (systolic blood pressure >140 mmHg, diastolic blood pressure >90 mmHg) and smokers were also excluded.

Animals

Previously reported PPAR α -deficient mice (*Ppara*^{-/-}) were used in these experiments.²³ All mice were 8 to 14 weeks old, and matched for weight and sex. Male ApoE-deficient (*ApoE*^{-/-}) mice (6 weeks old) were purchased from the Model Animal Research Center of Nanjing University (Nanjing, China). *Ppara*^{-/-}/*ApoE*^{-/-} mice were generated by cross-

ing *Ppara*^{-/-} and *ApoE*^{-/-} mice in the animal facilities of Zhejiang University. The animals were fed a normal chow diet until 8 weeks. Their diet was then switched to a high-fat diet, containing 40% fat and 1.25% cholesterol (Trophic Animal Feed High-Tech Co., Ltd, China), for 8 weeks. All animals were maintained under standard conditions of room temperature and humidity with a 12-hour dark-light cycle. All animal protocols were approved by Zhejiang University Laboratory Animal Welfare and Ethics Committee.

Preparation of washed human platelets

All blood donors had antecubital veins allowing a clean venipuncture. Blood was drawn without stasis into siliconized vacutainers containing 1/9 v/v 3.8% sodium citrate, then washed platelets were re-suspended as previously described.²⁴

Preparation of washed mice platelets

Whole blood was collected from the inferior vena cava into a 0.2 volume of ACD buffer (75 mM sodium citrate, 39 mM citric acid, and 135 mM dextrose, pH 6.5), and was diluted 1:3 with modified Tyrode buffer (20 mM HEPES, 137 mM NaCl, 13.8 mM NaHCO₃, 2.5 mM KCl, 0.36 mM NaH₂PO₄, 5.5 mM glucose, pH 7.4). Diluted whole blood was centrifuged at 180 g for 10 min at room temperature. The platelet-rich plasma was collected into a fresh tube containing 500 μ L ACD, and centrifuged at 700 g for 10 min. The platelet pellet was then re-suspended in modified Tyrode buffer.

Statistical analysis

Results are expressed as mean \pm standard error of the mean (SEM). Statistical significance was evaluated with a paired *t*-test, two-tailed Mann-Whitney U tests and two-way analysis of variance (ANOVA) using the statistical software GraphPad Prism (GraphPad Software, La Jolla, CA, USA).

Results

Ppara^{-/-} mice display impaired hemostasis and thrombosis

Ppara^{-/-} mice were genotyped by polymerase chain reaction and ablation of *Ppara* was confirmed in PPAR α -deficient platelets by western blot analysis (Figure 1A). The levels of expression of PPAR β and PPAR γ were similar in heterozygous (*Ppara*^{+/-}) platelets, *Ppara*^{-/-} platelets and wild-type (WT) platelets (Figure 1A). Moreover, *Ppara*^{-/-} mice were viable and fertile, and did not exhibit any evident bleeding tendency or thrombotic events over their lifespan. *Ppara*^{-/-} mice did not differ significantly from their WT littermates with regard to platelet count, red blood cell count, white blood cell count, hematocrit, or

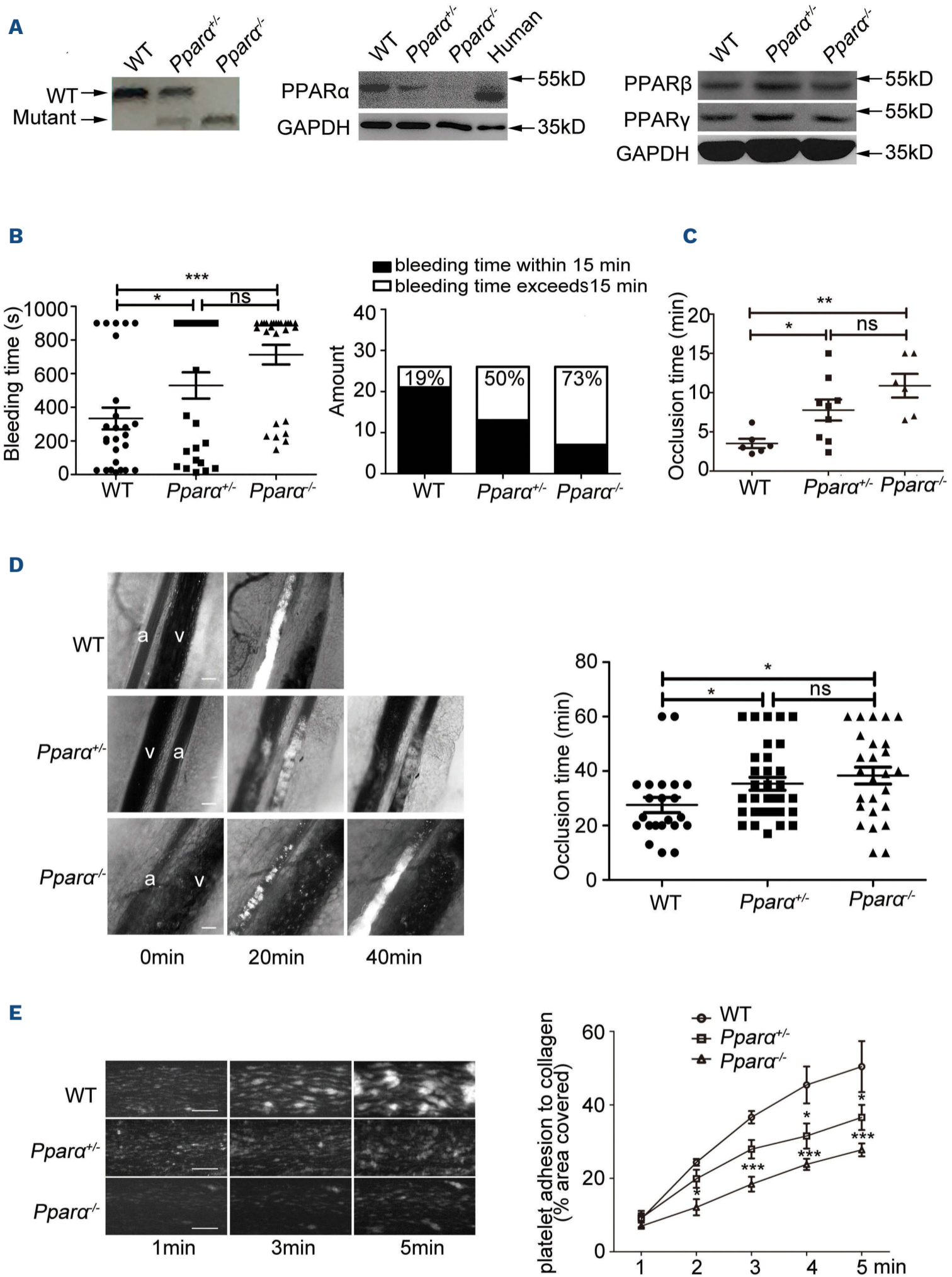


Figure 1. PPAR α -deficient mice display impaired hemostasis and thrombosis. (A) Genotyping results of wild-type (WT), *Ppara*^{+/-} and *Ppara*^{-/-} mice using polymerase chain reaction. Immunoblot analysis of PPAR α , PPAR β and PPAR γ expression in platelets from WT, *Ppara*^{+/-}, *Ppara*^{-/-} mice and humans. (B) Bleeding times for WT (●), *Ppara*^{+/-} (■) and *Ppara*^{-/-} (▲) mice. Means are indicated by horizontal lines. Statistical significance was evaluated with a paired *t* test (**P*<0.05; ****P*<0.001; ns: not significant). Percentages of WT, *Ppara*^{+/-} and *Ppara*^{-/-} mice bleeding times that exceeded 15 min (□) or were within 15 min (■). Results were obtained from 26 WT, 26 *Ppara*^{+/-} and 26 *Ppara*^{-/-} mice. (C) An injury to the carotid artery was induced by FeCl₃. The dot plot shows occlusion times for carotid arterioles as a result of FeCl₃-induced thrombosis in WT (●, n=6), *Ppara*^{+/-} (■, n=9) and *Ppara*^{-/-} mice (▲, n=6). Means are indicated by horizontal lines. Statistical significance was evaluated with a two-tailed Mann-Whitney test (**P*<0.05;

Legend on following page.

** $P < 0.01$; ns: not significant). (D) Representative images and time courses of thrombus formation induced by FeCl₃ injury to mesenteric arterioles in WT (top row), *Ppara*^{+/-} (middle row) and *Ppara*^{-/-} (bottom row) mice. a: arteriole; v: venule. Scale bars, 100 μ m (left panel). Dot plot showing occlusion times for arterioles as a result of FeCl₃-induced thrombosis in WT (●, n=22), *Ppara*^{+/-} (■, n=33) and *Ppara*^{-/-} mice (▲, n=26). Means are indicated by horizontal lines. Statistical significance was evaluated with a two-tailed Mann-Whitney test (* $P < 0.05$; ns: not significant). (E) Photomicrographs showing the progression of adhesion of platelets from WT, *Ppara*^{+/-} and *Ppara*^{-/-} mice on collagen. Whole blood from WT, *Ppara*^{+/-} and *Ppara*^{-/-} mice, collected in heparin (7.5 U/mL), was fluorescently labeled by incubation with mepacrine (100 μ M) for 30 min, and then perfused through fibrillar collagen-coated bioflux plates at a shear rate of 40 dynes/cm² for 5 min. Original magnification, $\times 10$. Scale bar, 100 μ m (left panel). Dot plot showing area coverage of platelets from WT (●), *Ppara*^{+/-} (■) and *Ppara*^{-/-} (▲) mice (n=3 for each group; two-way analysis of variance test, * $P < 0.05$; *** $P < 0.001$).

hemoglobin concentration (Online Supplementary Table S1). Electron microscopy showed normal discoid morphology of *Ppara*^{-/-} platelets with unaltered numbers of α granules and dense granules, compared to those in the WT platelets (Online Supplementary Figure S1A). No significant differences in the surface expression of platelet CD41 (α IIb subunit), and CD42b (GPIIb α subunit) were found between WT and *Ppara*^{-/-} platelets (Online Supplementary Figure S1B).

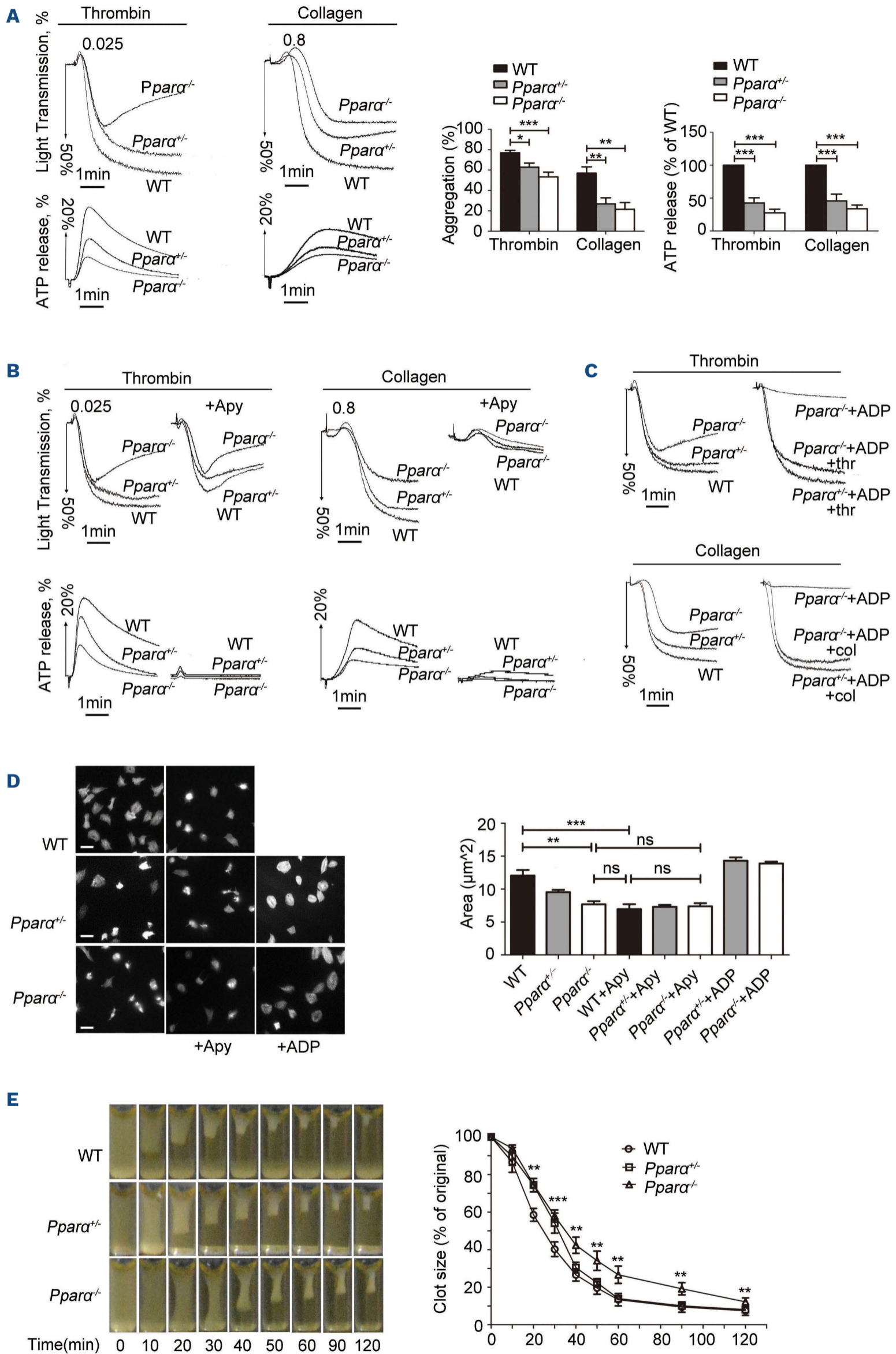
With a tail-bleeding assay, *Ppara*^{-/-} mice showed significantly prolonged tail bleeding time (712.80 \pm 58.11 seconds vs. 333.40 \pm 64.76 seconds; $P < 0.001$) (Figure 1B), agreeing with findings from a previous study.¹⁸ Moreover, 73% of the *Ppara*^{-/-} mice had a bleeding time exceeding 15 min, while the percentage in WT littermates was 19% (Figure 1B). In a FeCl₃-induced model of carotid artery thrombosis, the time to formation of a stable occlusive thrombus in the carotid artery was significantly longer in *Ppara*^{-/-} mice than in WT mice (10.88 \pm 1.51 min vs. 3.53 \pm 0.59 min, $P < 0.01$) (Figure 1C). In a FeCl₃-induced model of mesenteric arteriole thrombosis, the time to formation of stable occlusive thrombi was significantly longer in *Ppara*^{-/-} mice than in WT mice (38.35 \pm 3.10 min vs. 27.55 \pm 2.81 min, $P < 0.05$) (Figure 1D). Interestingly, heterozygous *Ppara*^{+/-} mice also had a significant perturbation of thrombotic and hemostatic functions, with significantly increased tail bleeding time, rate of non-stoppable bleeding, and time to the formation of stable occlusive thrombi compared to those of WT mice (Figure 1B-D). In a model of deep vein thrombosis, *Ppara*^{+/-} and *Ppara*^{-/-} mice developed thrombi similar in weight and length to those observed in WT mice (Online Supplementary Figure S2A, B), indicating a complex multi-cellular interaction upon PPAR α deficiency in thrombo-inflammation. These *in vivo* data indicate that PPAR α is essential for hemostasis and thrombosis, functions governed by platelets; nevertheless, the role of PPAR α is complicated in thrombo-inflammation because the outcome is dictated by the interaction of platelets and inflammatory cells.

In a microfluidic perfusion assay, when whole-blood was perfused over an immobilized collagen surface at the shear stress of 1000 s⁻¹ for 5 min, the areas covered by *Ppara*^{+/-} and *Ppara*^{-/-} platelets were 27.5% and 44.9% smaller in average than those by WT platelets (Figure 1E). A recombinant whole-blood system with diluted washed

platelets (2 \times 10⁷/mL) was used in the same assay to assess the collagen-adhesion ability of platelets. In the absence of platelet aggregation, the areas covered by collagen-adhered *Ppara*^{-/-} platelets were similar to those of WT platelets (Online Supplementary Figure S3). These findings indicate that PPAR α functions in regulating the growth of platelet thrombi, not the initial adhesion.

***Ppara*^{-/-} platelets show functional defects due to an impaired ATP secretion**

Next, platelet aggregation in response to common platelet stimuli was analyzed. Compared to WT platelets, *Ppara*^{-/-} platelets displayed an average 30% reduction of aggregation rates in response to thrombin (0.025 U/mL) and 57% reduction in response to collagen (0.8 μ g/mL) (Figure 2A). However, ADP and TXA₂ analog U46619-induced platelet aggregation was not affected by PPAR α deficiency (Online Supplementary Figure S4A). Although dense granule content was normal in *Ppara*^{-/-} platelets (Online Supplementary Figure S4B), ATP release induced by low doses of thrombin (0.025 U/mL), collagen (0.8 μ g/mL) and U46619 (0.3 μ M) was largely inhibited in *Ppara*^{-/-} platelets (Figure 2A and Online Supplementary Figure S4A). Again, *Ppara*^{+/-} platelets exhibited intermediate rates of aggregation and dense granule secretion (Figure 2A). Higher concentrations of thrombin (0.05 U/mL) and collagen (2 μ g/mL) overcame the defective aggregation and dense granule secretion in *Ppara*^{-/-} platelets (Online Supplementary Figure S4A). The aggregation differences between WT and *Ppara*^{-/-} platelets were abolished when apyrase was applied to hydrolyze dense granule-secreted ATP and ADP (Figure 2B and Online Supplementary Figure S4C). Conversely, supplementation with a low concentration of ADP (1 μ M), which was insufficient to induce aggregation on its own, rescued the defective aggregation of *Ppara*^{+/-} and *Ppara*^{-/-} platelets stimulated by thrombin or collagen (Figure 2C and Online Supplementary Figure S4D). As indicated by the measurement of TXB₂, collagen- or thrombin-induced TXA₂ production was comparable between WT and *Ppara*^{-/-} platelets (Online Supplementary Figure S4E). Moreover, the secretion of α -granules and activation of α IIb β 3, measured respectively by P-selectin expression and the binding of Jon/A antibody, were not influenced by PPAR α deficiency in response to thrombin and convulxin (Online Supplementary Figure S4F). These data suggest that the impaired



Legend on following page.

Figure 2. Ppara^{-/-} platelets show impaired aggregation, ATP secretion, spreading and delayed clot retraction. (A) Aggregation and ATP release of washed wild-type (WT), Ppara^{+/-} and Ppara^{-/-} platelets stimulated with thrombin (0.025 U/mL) or collagen (0.8 μ g/mL). Aggregation and ATP release were assessed with a Chrono-log lumiaggregometer under stirring at 1,200 rpm. Traces are representative of at least three independent experiments. Statistical significance was evaluated with a two-tailed Mann-Whitney test and a paired *t* test (**P*<0.05; ***P*<0.01; ****P*<0.001). (B) Aggregation and ATP release of washed WT, Ppara^{+/-} and Ppara^{-/-} platelets stimulated with thrombin (0.025 U/mL) or collagen (0.8 μ g/mL) in the presence of vehicle or apyrase (1 U/mL) incubated for 5 min. Traces are representative of at least three independent experiments. (C) Aggregation of washed WT, Ppara^{+/-} and Ppara^{-/-} platelets stimulated with thrombin (0.025 U/mL) or (0.8 μ g/mL) in the presence of a low concentration of ADP (1 μ M). Traces are representative of at least three independent experiments. (D) Spreading of WT, Ppara^{+/-} and Ppara^{-/-} platelets on immobilized fibrinogen in the presence or absence of apyrase (1 U/mL) or ADP (1 μ M). Images are representative of three independent experiments with similar results. Original magnification, \times 100. Scale bar, 10 μ m (left panel). Statistical significance was evaluated with a two-tailed Mann-Whitney test (***P*<0.01; ****P*<0.001; ns: not significant). (E) Platelets from WT, Ppara^{+/-} and Ppara^{-/-} mice were resuspended with human platelet-poor plasma at a concentration of 4×10^8 /mL, and recombined plasma was stimulated to coagulate with thrombin (0.4 U/mL), then photographed at different time points. Statistical significance was evaluated with a paired *t* test (**P*<0.05; ***P*<0.01).

aggregation in Ppara^{-/-} platelets is caused by the reduced ADP secretion. Consistent with the role of ADP in thrombus amplification, Ppara^{-/-} platelets formed smaller aggregates than WT platelets when stimulated with low doses of thrombin and collagen (*Online Supplementary Figure S4G*).

Platelet spreading on immobilized fibrinogen and clot retraction, two processes controlled by early and late integrin α IIb β 3-mediated outside-in signaling, respectively, were then measured. Platelet spreading on immobilized fibrinogen (Figure 2D) and clot retraction (Figure 2E) were also inhibited by PPAR α deficiency. Apyrase eliminated the spreading difference between WT and Ppara^{-/-} platelets, and exogenous ADP (1 μ M) rescued the defective spreading of Ppara^{-/-} platelets (Figure 2D). Clot retraction mediated by Ppara^{-/-} platelets showed a significant delay compared to that by WT platelets (Figure 2E). These data demonstrate an important role for PPAR α in platelet dense granule secretion and its activation.

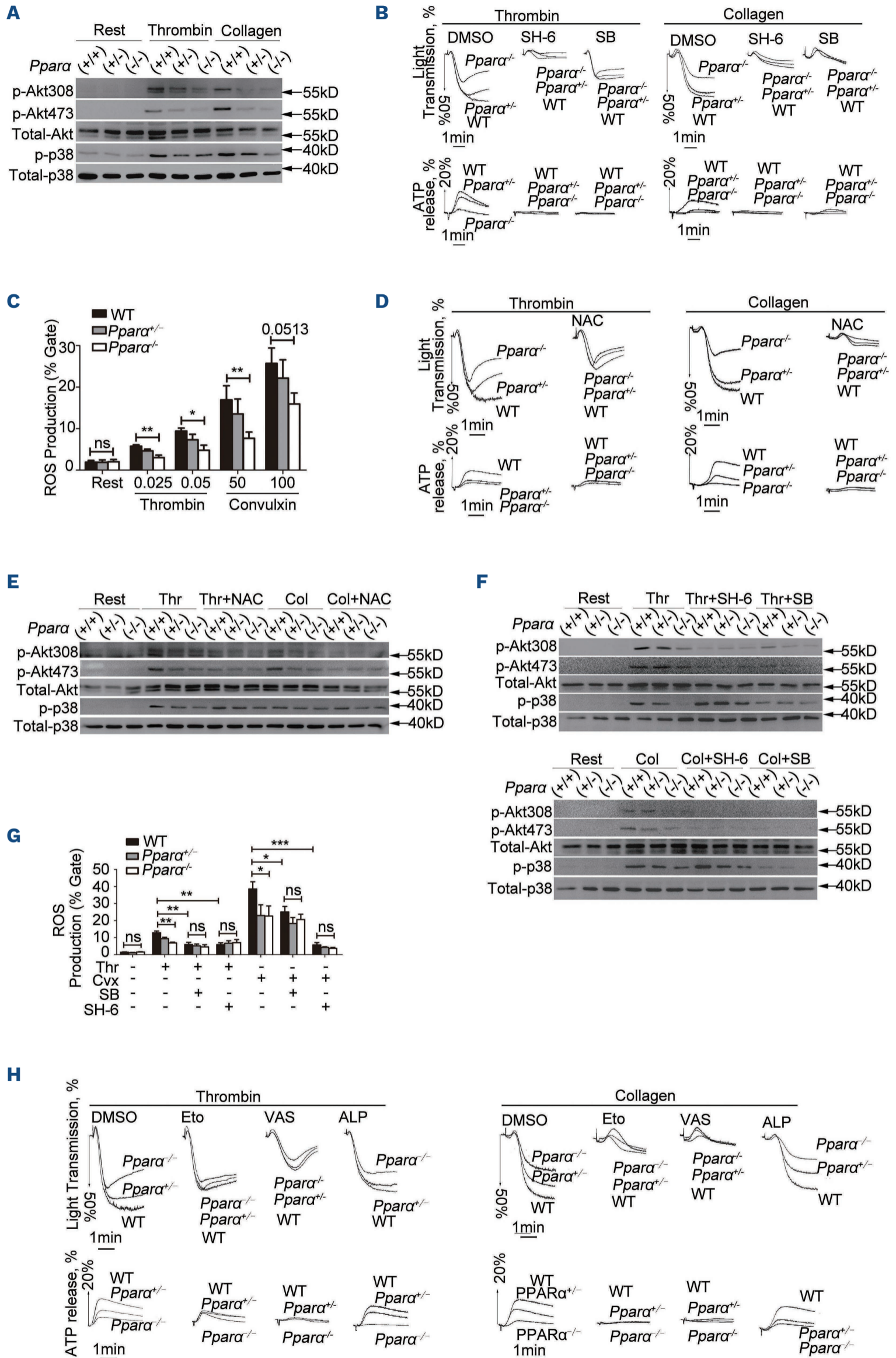
PPAR α promotes platelet activation through a p38/ROS/Akt signal axis

When platelet signaling events were analyzed, both collagen and thrombin induced a significantly reduced phosphorylation of Akt (Thr³⁰⁸/Ser⁴⁷³) and p38 (Thr¹⁸⁰/Tyr¹⁸²) in Ppara^{-/-} platelets (Figure 3A and *Online Supplementary Figure S5A*), while phosphorylation of ERK1/2 (Thr²⁰²/Tyr²⁰⁴) and JNK (Thr¹⁸³/Tyr¹⁸⁵) remained unaltered (*Online Supplementary Figure S5A*). Moreover, both SB203580 and SH-6, inhibitors of p38 and Akt, strongly inhibited platelet aggregation and ATP release induced by thrombin and collagen, but no additive effects with PPAR α deficiency were observed (Figure 3B and *Online Supplementary Figure S5B*). Therefore, PPAR α is functionally coupled to p38 and Akt activation. As p38 regulates the production of ROS,^{25,26} thrombin and convulxin induced significantly less ROS production in Ppara^{+/-} and Ppara^{-/-} platelets than in WT platelets (Figure 3C), while ROS scavenging by *N*-acetylcysteine (NAC) essentially eliminated the aggregation and ATP release difference among WT, Ppara^{+/-}, and Ppara^{-/-} platelets (Figure 3D and *Online Supplementary Figure S5C*).

Intriguingly, NAC treatment abolished the difference of Akt phosphorylation but left intact the difference of p38 phosphorylation among WT, Ppara^{+/-} and Ppara^{-/-} (Figure 3E and *Online Supplementary Figure S6A*). Furthermore, SB203580 and SH-6 eliminated the differences of Akt phosphorylation (Figure 3F and *Online Supplementary Figure S6B*) and ROS production (Figure 3G) between WT and Ppara^{-/-} platelets; whereas SH-6 did not change the phosphorylation of p38 (Figure 3F and *Online Supplementary Figure S6B*). These data suggest a sequential relay of PPAR α , p38, ROS production, and Akt during platelet activation.

Sources of ROS were also investigated using the NADPH oxidase inhibitor VAS2780, CPT-I inhibitor etomoxir, and xanthine oxidase inhibitor allopurinol (*Online Supplementary Figure S6C*). VAS2780 and etomoxir, but not allopurinol, eliminated the differences of platelet aggregation and ATP release between WT and Ppara^{-/-} platelets (Figure 3H and *Online Supplementary Figure S6D*). Both VAS2780 and etomoxir eliminated the phosphorylation difference of Akt, but not that of p38 between WT and Ppara^{-/-} platelets (*Online Supplementary Figure S6E*). These data suggest that ROS from NADPH oxidase and mitochondrial fatty acid β -oxidation constitute the important sources of ROS for PPAR α -regulated platelet activation.

Consistent with previous reports,^{18,19} a synthetic PPAR α agonist WY14643 inhibited aggregation and ATP release induced by low doses of thrombin and collagen in WT platelets (*Online Supplementary Figure S7A*), and essentially abolished the differences between WT and Ppara^{-/-} platelets (*Online Supplementary Figure S7A*). Unexpectedly, a PPAR α antagonist GW6471 also inhibited aggregation and ATP release in WT platelets and eliminated the difference between WT and Ppara^{-/-} platelets in response to low doses of thrombin and collagen (*Online Supplementary Figure S7B*). WY14643 and GW6471 both inhibited phosphorylation of Akt Ser⁴⁷³ upon platelet activation by collagen, indicating that these compounds act by interrupting PPAR α signaling in platelets (*Online Supplementary Figure S7C*). Moreover, GW6471 *per se* but not WY14643 induced phosphorylation of Akt Ser⁴⁷³ (*Online Supplementary Figure*



Legend on following page.

Figure 3. PPAR α promotes platelet activation through a p38/ROS/Akt signal axis. (A) Immunoblot analysis of wild-type (WT), *Ppara*^{+/-} and *Ppara*^{-/-} platelets, stimulated with thrombin (0.025 U/mL) and collagen (0.8 μ g/mL) for 5 min, with antibodies recognizing phosphorylated Akt Thr³⁰⁸, phosphorylated Akt Ser⁴⁷³, total Akt, phosphorylated p38 Thr¹⁸⁰/Tyr¹⁸² (T¹⁸⁰/Y¹⁸²), and total p38. Representative immunoblots from at least three independent experiments. (B) Washed WT, *Ppara*^{+/-} and *Ppara*^{-/-} platelets (2 \times 10⁸/mL) were incubated with dimethyl sulfoxide (DMSO), SH-6 (10 μ M), SB203580 (10 μ M) for 10 min, then stimulated with thrombin (0.025 U/mL) or collagen (0.8 μ g/mL), respectively. Aggregation and ATP release were assessed with a Chrono-log lumiaggregometer under stirring at 1,200 rpm. Traces are representative of at least three independent experiments. (C) Generation of reactive oxygen species (ROS) analyzed by flow cytometry. H2DCFDA-loaded (50 μ M) mice platelets were stimulated with thrombin (0.025 and 0.05 U/mL) or convulxin (50 and 100 ng/mL) for 5 min. Samples were analyzed immediately. Statistical significance was evaluated with a two-tailed Mann-Whitney test (**P*<0.05; ***P*<0.01; ns: not significant). (D) Washed WT, *Ppara*^{+/-} and *Ppara*^{-/-} platelets (2 \times 10⁸/mL) were incubated with or without N-acetylcysteine (NAC, 2 mM) for 5 min, then stimulated with thrombin (0.025 U/mL) or collagen (0.8 μ g/mL), respectively. Aggregation and ATP release were assessed with a Chrono-log lumiaggregometer under stirring at 1,200 rpm. Traces are representative of at least three independent experiments. (E) Immunoblot analysis of WT, *Ppara*^{+/-} and *Ppara*^{-/-} platelets stimulated with thrombin (0.025 U/mL) and collagen (0.8 μ g/mL) for 5 min in the absence or presence of NAC, with antibodies recognizing phosphorylated Akt Thr³⁰⁸, phosphorylated Akt Ser⁴⁷³, total Akt, phosphorylated p38 Thr¹⁸⁰/Tyr¹⁸² (T¹⁸⁰/Y¹⁸²), and total p38. Representative immunoblots from at least three independent experiments. (F) Immunoblot analysis of WT, *Ppara*^{+/-} and *Ppara*^{-/-} platelets, stimulated with thrombin (0.025 U/mL) or collagen (0.8 μ g/mL) for 5 min in the presence of DMSO, SH-6 (10 μ M), and SB203580 (10 μ M), with antibodies recognizing phosphorylated Akt Thr³⁰⁸, phosphorylated Akt Ser⁴⁷³, total Akt, phosphorylated p38 Thr¹⁸⁰/Tyr¹⁸² (T¹⁸⁰/Y¹⁸²), and total p38. Representative immunoblots from at least three independent experiments. (G) H2DCFDA-loaded (50 μ M) mice platelets were incubated with DMSO, SH-6 (10 μ M) or SB203580 (10 μ M), stimulated with thrombin (0.05 U/mL) or convulxin (100 ng/mL) for 5 min. Samples were analyzed immediately. Statistical significance was evaluated with a two-tailed Mann-Whitney test (**P*<0.05; ***P*<0.01; ****P*<0.001; ns: not significant). (H) Washed WT, *Ppara*^{+/-} and *Ppara*^{-/-} platelets (2 \times 10⁸/mL) were incubated with DMSO, etomoxir (25 μ M), VAS2870 (10 μ M), or ALP (200 μ M) for 10 min, then stimulated with thrombin (0.025 U/mL) or collagen (0.8 μ g/mL), respectively. Aggregation and ATP release were assessed with a Chrono-log lumiaggregometer under stirring at 1,200 rpm. Traces are representative of at least three independent experiments.

S7D). Therefore, GW6471 may be a partial agonist in the context of platelet activation. Hence, the agonist and antagonist of PPAR α both appear to inhibit platelet function, possibly due to the disruption of signal transduction mediated by PPAR α .

PPAR α mediates hyperlipidemia-associated prothrombotic status and oxidized low-density lipoprotein-evoked platelet activation

Consistent with the previous study,²⁷ after 8 weeks of a high-fat diet, total plasma levels of cholesterol and triglycerides in *Ppara*^{+/-}/*ApoE*^{-/-} mice were significantly increased, while they did not undergo further change in *Ppara*^{-/-}/*ApoE*^{-/-} mice (*Online Supplementary Table S2*). The occlusion time in FeCl₃-induced mesenteric arteriole thrombosis in *Ppara*^{+/-}/*ApoE*^{-/-} mice was significantly shortened by a high-fat diet when compared with the control diet. But it was comparable between *Ppara*^{-/-}/*ApoE*^{-/-} mice fed with a high-fat diet and *Ppara*^{+/-}/*ApoE*^{-/-} mice fed the control diet (Figure 4A).

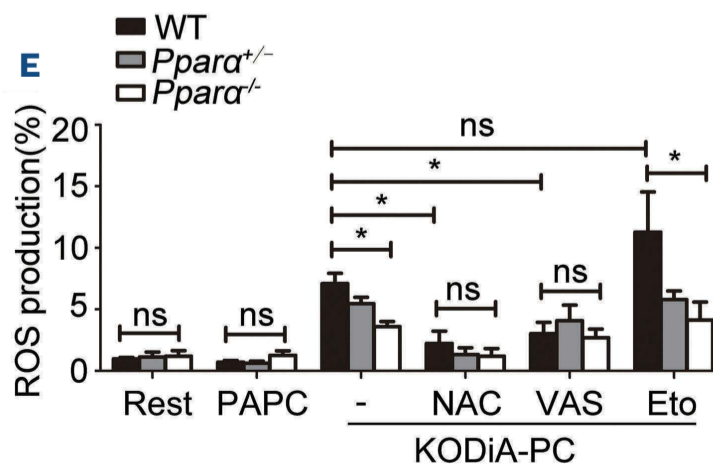
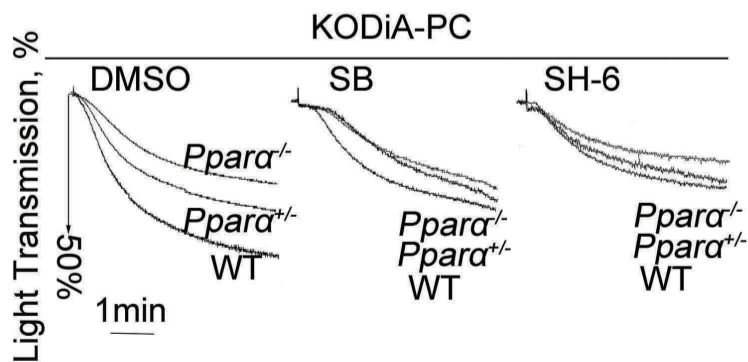
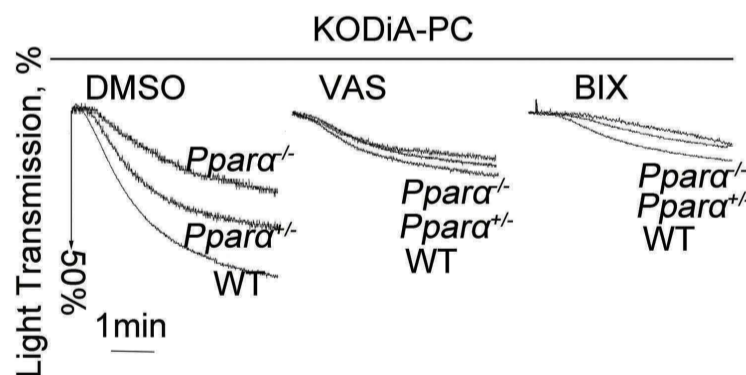
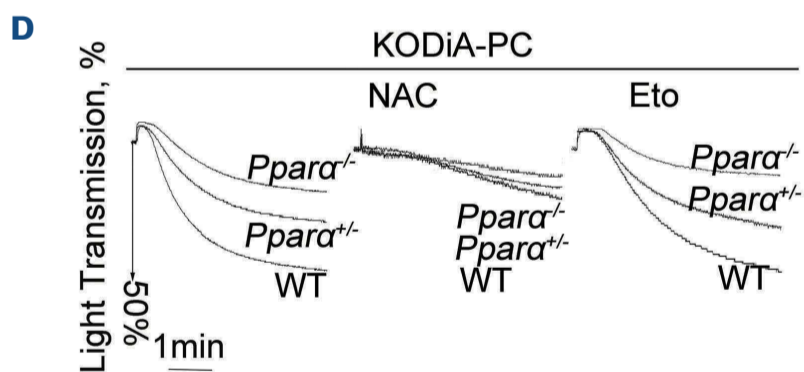
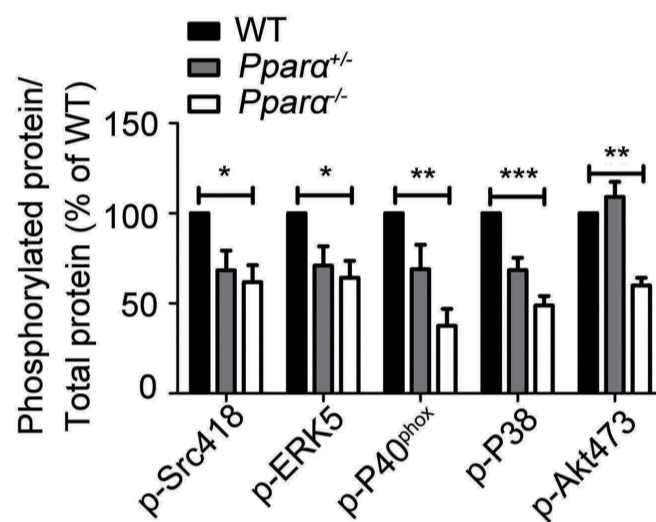
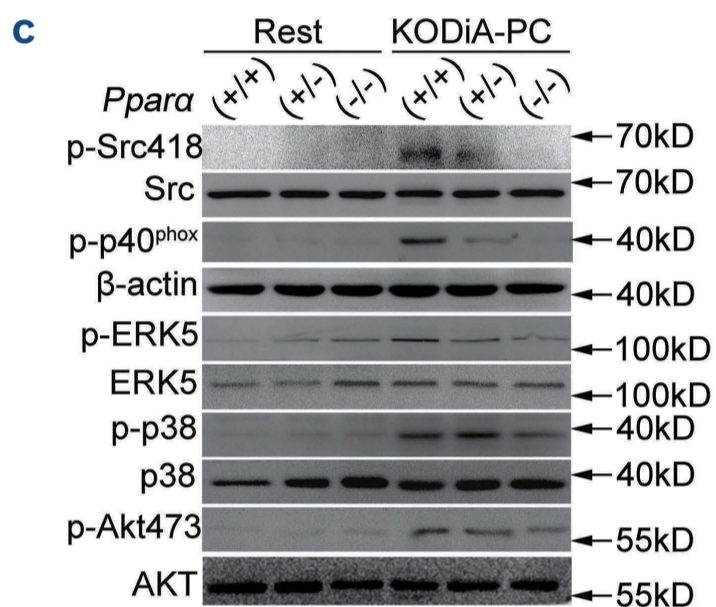
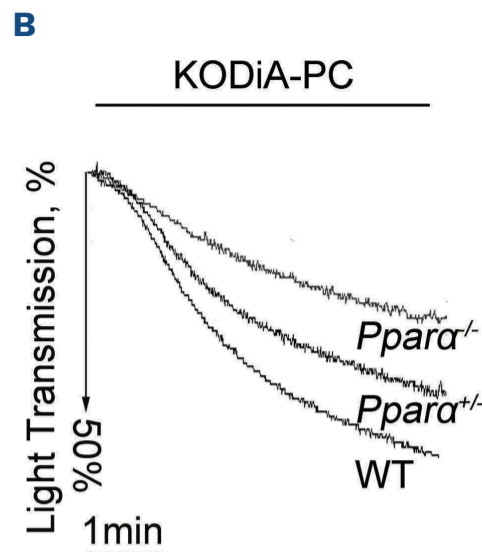
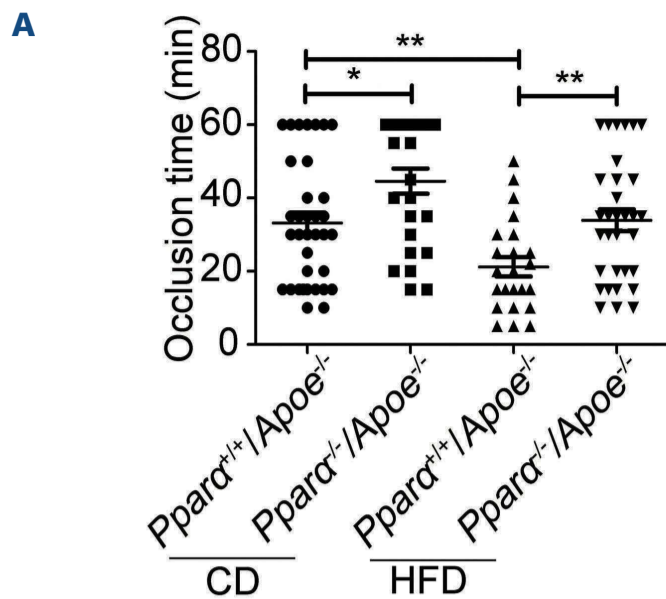
KODiA-PC, 1-(palmitoyl)-2-(5-keto-6-octene-diyl) phosphatidylcholine, one of the most potent CD36 ligands in the oxLDL species, caused direct platelet aggregation, which was largely decreased in *Ppara*^{-/-} platelets (Figure 4B and *Online Supplementary Figure S8A*). Consistently, KODiA-PC induced a significantly reduced phosphorylation of Src (Tyr⁴¹⁸), p40^{phox} and ERK5 (Thr²¹⁸/Tyr²²⁰), Akt (Ser⁴⁷³) and p38 (Thr¹⁸⁰/Tyr¹⁸²) in *Ppara*^{-/-} platelets, compared with WT platelets (Figure 4C). Moreover, the NADPH oxidase inhibitor VAS2780, the ROS scavenger NAC, the ERK5 inhibitor BIX02188, the p38 inhibitor SB203580 and the Akt inhibitor SH-6, but not the CPT-I inhibitor etomoxir, elimi-

nated the difference in aggregation between WT and *Ppara*^{-/-} platelets (Figure 4D and *Online Supplementary Figure S8B*). Robust ROS production induced by KODiA-PC was also reduced by PPAR α deficiency (Figure 4E). Interestingly, ROS production by KODiA-PC was inhibited by VAS2780 and NAC, but not etomoxir (Figure 4E). These data indicate that PPAR α mediates oxLDL-induced platelet activation, which is associated with an altered ROS generation pathway.

Platelet PPAR α expression correlates with platelet hyperreactivity

Having established the importance of PPAR α in hyperlipidemic-induced platelet activation, we further found that PPAR α expression in platelets was significantly increased in mice fed a high-fat diet, compared to that in mice fed with a control diet (Figure 5A). The expression of platelet PPAR β and PPAR γ was however not significantly influenced by the high-fat diet (Figure 5A). In mice fed a high-fat diet, the increase of PPAR α expression was accompanied by an increase in platelet aggregation induced by thrombin and collagen (Figure 5B and *Online Supplementary Figure S9*). These data indicate that increased platelet PPAR α expression in hyperlipidemic mice is responsible for platelet hyperactivity.

Platelet PPAR α expression was also determined in healthy volunteers and patients with hyperlipidemia (*Online Supplementary Table S3*). Platelet PPAR α protein and mRNA levels were significantly increased in patients with hypertriglyceridemia and hypercholesterolemia (Figure 5C, D), although the expression of PPAR β and PPAR γ proteins was similar in healthy subjects and hyperlipidemic patients (Fi-



Legend on following page.

Figure 4. PPAR α mediates hyperlipidemia-associated prothrombotic status and oxLDL-evoked platelet activation. (A) *Ppara*^{+/+}/*ApoE*^{-/-} and *Ppara*^{-/-}/*ApoE*^{-/-} mice were fed a high-fat diet (HFD) or control diet (CD) for 8 weeks before undergoing *in vivo* thrombosis experiments. Platelets were labeled by direct tail vein injection of DiOC6 (10 μ M, 100 μ L). Dot plot showing occlusion times for arterioles as a result of FeCl₃-induced thrombosis in *Ppara*^{+/+}/*ApoE*^{-/-} and *Ppara*^{-/-}/*ApoE*^{-/-} mice. Means are indicated by horizontal lines. Statistical significance was evaluated with a two-tailed Mann-Whitney test (* P <0.05; ** P <0.01). (B) Platelets were stimulated with 1-(palmitoyl)-2-(5-keto-6-octenedioyl) phosphatidylcholine (KODiA-PC, 15 μ M). Aggregation was assessed with a Chrono-log lumiaggregometer under stirring at 1,200 rpm. Traces are representative of at least three independent experiments. (C) Immunoblot analysis of wild-type (WT), *Ppara*^{+/+} and *Ppara*^{-/-} platelets stimulated with KODiA-PC for 5 min, with antibodies recognizing phosphorylated Src Tyr⁴¹⁸ (Y418), total Src, phosphorylated p40phox, β -actin, phosphorylated ERK5 Thr²¹⁸/Tyr²²⁰ (T218/Y220), total ERK5, phosphorylated p38, total p38, phosphorylated Akt Ser473, and total Akt (top panel). Statistical significance was evaluated with a paired Student t test (* P <0.05; ** P <0.01; *** P <0.001) (bottom panel). (D) Washed WT, *Ppara*^{+/+} and *Ppara*^{-/-} platelets were incubated with N-acetylcysteine (NAC, 2 mM), etomoxir (Eto, 25 μ M), dimethylsulfoxide (DMSO), VAS2870 (10 μ M), BIX02188 (10 μ M), SB203580 (10 μ M), or SH-6 (10 μ M) for 10 mins, then stimulated with KODiA-PC (15 μ M). Aggregation was assessed with a Chrono-log lumiaggregometer under stirring at 1,200 rpm. Traces are representative of at least three independent experiments. (E) H2DCFDA-loaded (50 μ M) mice platelets were incubated with DMSO, NAC (2 mM), VAS2870 (10 μ M), or etomoxir (25 μ M), stimulated with KODiA-PC (15 μ M) for 10 min. PAPC was used as a negative control. Samples were analyzed immediately. Statistical significance was evaluated with a two-tailed Mann-Whitney test (* P <0.05; ns: not significant).

Figure 5C). As expected, platelet aggregation in response to thrombin was enhanced in patients with hypertriglyceridemia or hypercholesterolemia compared to that in healthy subjects (Figure 5E). The level of platelet PPAR α expression was closely correlated with platelet aggregation in response to thrombin (Figure 5F). These findings demonstrate that the increased expression of platelet PPAR α in patients with hyperlipidemia is closely related to platelet activity.

Oxidized low-density lipoproteins and lipids upregulate megakaryocyte- but not platelet- PPAR α

Compared with platelets treated with normal medium, platelets incubated with a fatty acid (oleic acid or palmitic acid), cholesterol or oxLDL for 12 h or 24 h did not alter the PPAR α levels (*Online Supplementary Figure S10A*). In contrast, PPAR α protein and mRNA levels in Meg-01 cells were significantly increased after 24 h incubation with the fatty acid, cholesterol or oxLDL (Figure 6A, B and *Online Supplementary Figure S10B*), without a concomitant change of the expression of PPAR β and PPAR γ (Figure 6A and *Online Supplementary Figure S10B*). These data suggest that the increased PPAR α in hyperlipidemic platelets may derive from megakaryocytes.

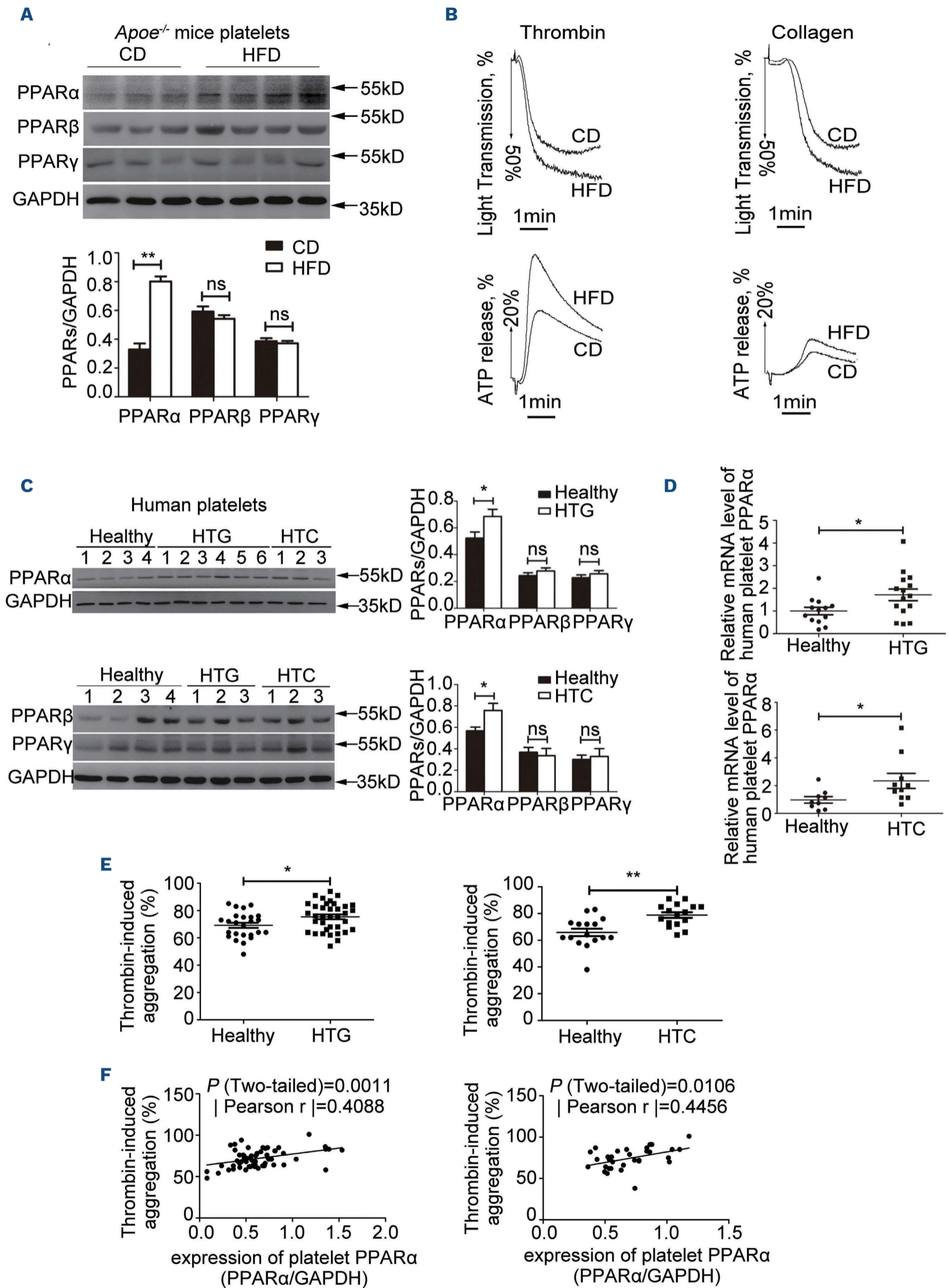
It was reported that hyperlipidemia induces ROS generation and activation of the NF- κ B signaling pathway.²⁸ Indeed, treating Meg-01 cells with the NF- κ B inhibitor BAY11-7082, antioxidants NAC or DTT, abolished the PPAR α upregulation by fatty acids, cholesterol or oxLDL (Figure 6C, D and *Online Supplementary Figure S10C*). Moreover, BAY11-7082 and NAC or DTT inhibited fatty acid-, cholesterol- or oxLDL-induced phosphorylation of I κ B α (Figure 6C, D and *Online Supplementary Figure S10C*). An *in silico* promoter analysis (Jaspar and ensemble Genome Browser) identified the possible NF- κ B-binding sites on the *Ppara* promoter. Four potential NF- κ B sites in the sense strand of the region -105/-114 bp (region 1), -168/-177 bp (region 2), -1588/-1597 bp (region 3) and -1878/-1887 bp (region 4). Chromatin immunoprecipitation analyses revealed a mar-

ked binding of p65 to region 1 of the *Ppara* promoter of megakaryocytes when treated with fatty acid, cholesterol or oxLDL (Figure 6E), indicating that NF- κ B directly regulates *Ppara* transcription in Meg-01 cells. Thus, fatty acids, cholesterol or oxLDL upregulate PPAR α expression in Meg-01 cells through ROS and subsequent NF- κ B signaling.

Discussion

The present study investigated the role of PPAR α in platelet activation and the impact of PPAR α in the prothrombotic potential caused by hyperlipidemia. The results demonstrated that PPAR α is an indispensable signaling molecule supporting platelet activation and thrombosis. Importantly, increased PPAR α expression in platelets is responsible for enhanced platelet activity by hyperlipidemia. Hyperlipidemia does not trigger PPAR α expression in platelets directly, but rather does so in megakaryocytes through ROS and NF- κ B pathways. Our study not only elucidated the signaling function of PPAR α in supporting platelet activation, but also revealed a key role for PPAR α in bridging the genetic effect of hyperlipidemia on megakaryocytes with the prothrombotic potential operated by platelets.

This study clearly demonstrated the positive role that PPAR α serves in supporting platelet activation and thrombosis. However, previous studies showed some synthetic^{18,19} or endogenous molecules¹⁹ inhibited platelet activation and thrombosis in a PPAR α -dependent manner. This discrepancy may suggest the existence of endogenous PPAR α ligands which serve as a positive regulator of platelet function and thrombosis. Although such ligands of PPAR α have yet to be defined, given the phenotype of platelets upon PPAR α deficiency, it is possible that these stimulatory ligands are the ones playing dominant roles in platelet activation. While lipids with cardioprotective effects (e.g., polyunsaturated fatty acids)²⁹ are able to produce endogenous PPAR α ligand with platelet-inhibitory



Legend on following page.

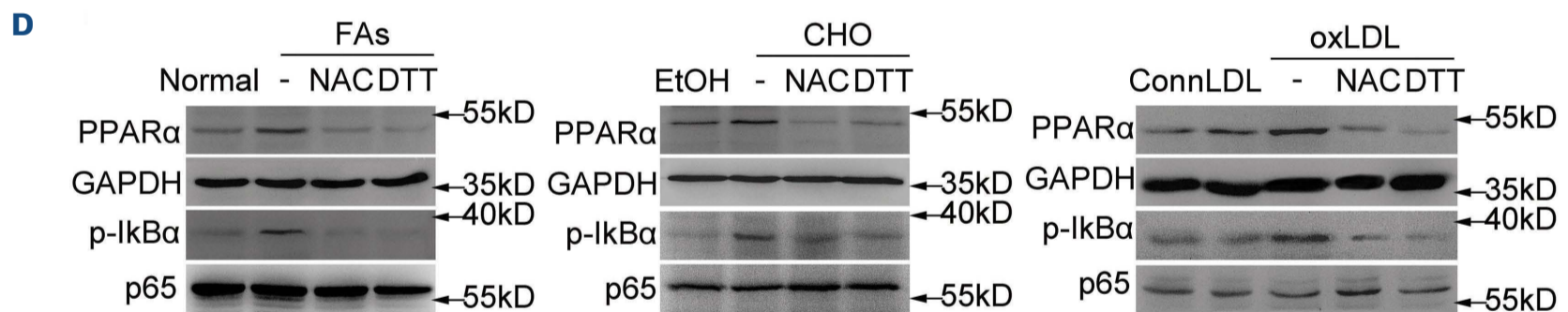
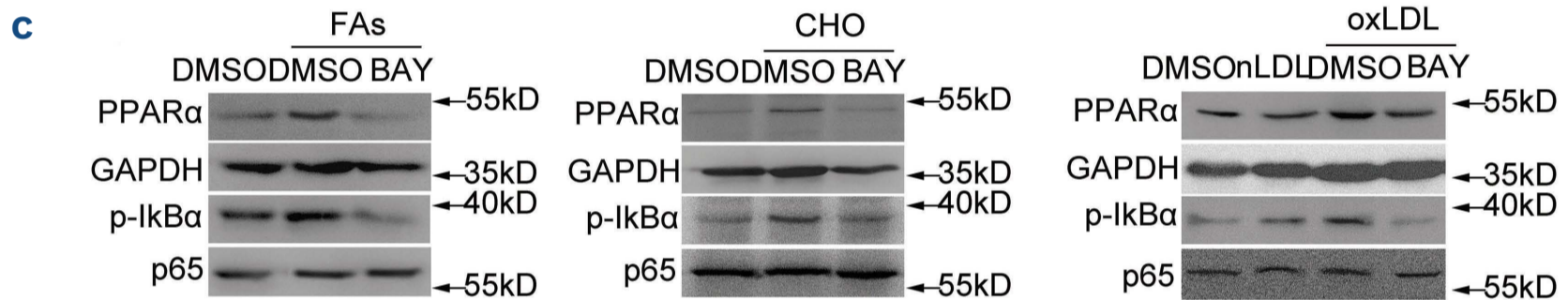
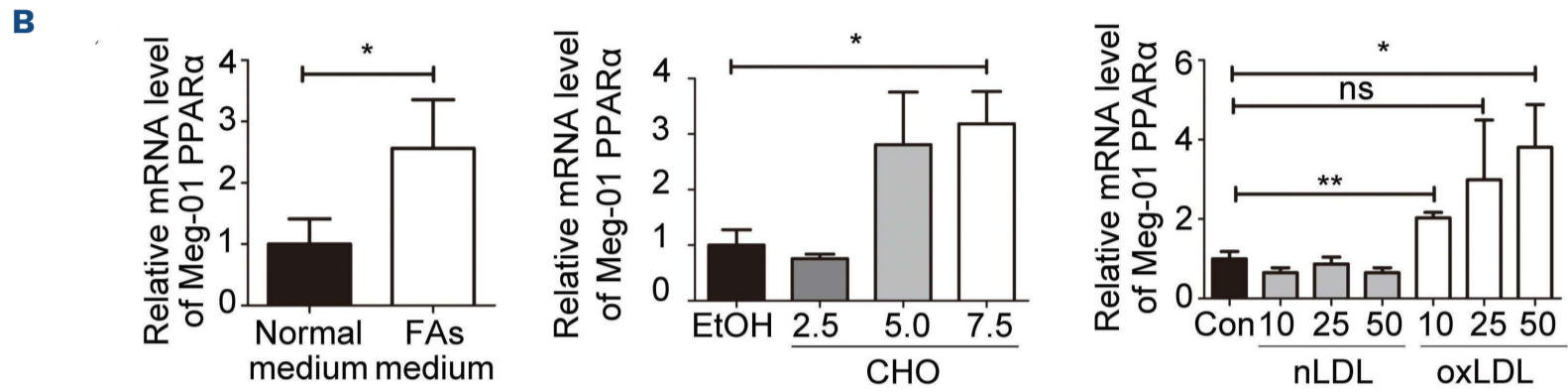
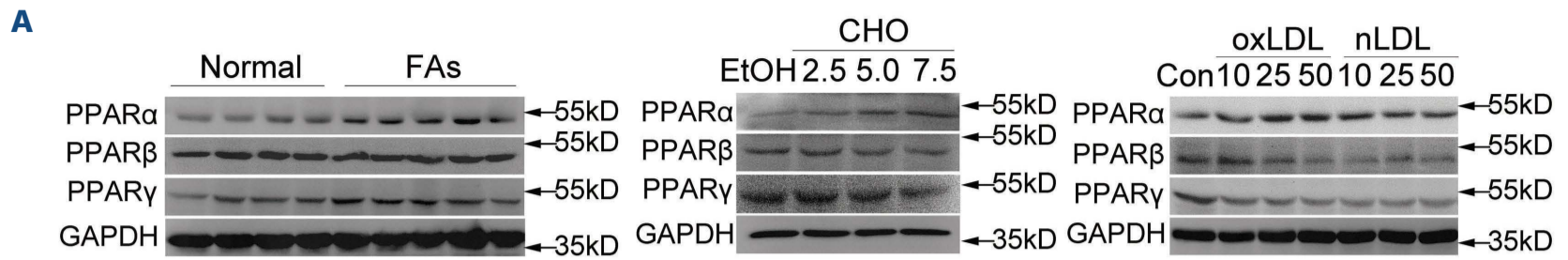
Figure 5. Increased platelet PPAR α expression correlates with platelet hyperreactivity in hyperlipidemic mice and patients with hyperlipidemia. (A) Immunoblot analysis of PPAR α , PPAR β and PPAR γ expression in platelets from *Apoe*^{-/-} mice fed a high-fat diet (HFD) or control diet (CD) for 8 weeks with PPAR α , PPAR β and PPAR γ antibodies. Statistical significance was evaluated with a two-tailed Mann-Whitney test (***P*<0.01; ns: not significant). (B) Aggregation and ATP release of platelets from *Apoe*^{-/-} mice fed with a HFD or CD were stimulated with thrombin (0.015 U/mL) or collagen (0.6 μ g/mL). Aggregation was assessed with a Chrono-log lumiaggregometer under stirring at 1,200 rpm. Traces are representative of at least three independent experiments. (C) Immunoblot analysis of PPAR α , PPAR β and PPAR γ expression in platelets from patients with hypertriglyceridemia (HTG) and hypercholesterolemia (HTC) with PPAR α , PPAR β and PPAR γ antibodies. Representative immunoblots of platelet PPAR α and glyceraldehyde 3-phosphate dehydrogenase (GAPDH) from four healthy subjects, six patients with HTG and three patients with HTC. Representative immunoblots of platelet PPAR β , PPAR γ and GAPDH from four healthy subjects, three patients with HTG and three patients with HTC. Statistical significance was evaluated with a two-tailed Mann-Whitney test (**P*<0.05; ns: no significance). (D) *PPARA* mRNA expression in platelets from healthy subjects (n=10) and patients with HTG (n=12) or healthy subjects (n=9) and patients with HTC (n=10) was analyzed by quantitative real-time polymerase chain reaction. Statistical significance was evaluated with a two-tailed Mann-Whitney test (**P*<0.05). (E) Aggregation of platelets from healthy subjects (n=25) and patients with HTG (n=36) or healthy subjects (n=16) and patients with HTC (n=16) in response to thrombin (0.025 U/mL). Aggregation was assessed with a Chrono-log lumiaggregometer under stirring at 1,200 rpm. Statistical significance was evaluated with a two-tailed Mann-Whitney test (**P*<0.05). (F) Platelet aggregation induced by thrombin is well correlated with protein level of platelet PPAR α expression in healthy subjects (n=25) and patients with HTG (n=36) or healthy subjects (n=16) and patients with HTC (n=16). Each solid circle represents a different individual (Pearson correlation, GraphPad Prism 5).

properties (e.g., DPAn-6),¹⁹ lipid species with cardiovascular disease-promoting properties, such as saturated fatty acids,²⁹ may generate derivatives which serve as stimulatory PPAR α ligands to promote platelet activation. Identification of the stimulatory ligands may thus provide novel targets for the intervention of thrombosis and constitutes an important theme in its own right. Moreover, based on the fact that ligands mainly target the ligand-binding domain of PPAR α ,^{30,31} it is tempting to hypothesize that a conformational change induced by occupancy of the region of the ligand-binding domain may be key to the nongenomic function of PPAR α . Future structural studies are therefore imperative to provide further insight into this promising anti-thrombotic target.

This study not only confirmed that the key contribution of PPAR α to thrombosis and hemostasis is through the regulation of platelet dense granule secretion, but also revealed the pathway on which PPAR α relies to perform its function. Hence, p38 and Akt were identified as the sequential signals downstream of PPAR α to regulate platelet dense granule secretion. These findings are in agreement with the previously reported roles of p38 and Akt in platelets. For example, p38 has been shown to positively regulate dense granule secretion,²⁵ and Akt have also been reported to be important in dense granule secretion through promoting nitric oxide/cGMP signaling³² or inhibiting GSK3 β .³³ Moreover, our results suggest that p38 activation is relayed by Akt phosphorylation, which is also consistent with a previous report.³⁴ Given the intact Jon/A binding and the significantly reduced spreading on immobilized fibrinogen upon PPAR α deficiency, it seems that PPAR α mainly participates in outside-in signaling rather than inside-out signaling. This observation is also consistent with previous reports, which suggested that outside-in signaling and dense granule secretion are coupled and both are regulated by p38 and Akt signaling, evidenced by the studies employing either inhibition or genetic

ablation of p38 or Akt.^{25,32} Downstream of p38, ROS generation has been found to be a pivotal link between PPAR α and platelet activation, echoing a previous finding in macrophages.³⁵ It seems that hemostatic stimuli³⁶⁻³⁸ and oxLDL⁹ may differentially employ the ROS generation pathways. Notably, our data indicate that PPAR α critically contributes to the generation of ROS controlled by both mitochondrial fatty acid β -oxidation and NADPH oxidases. Therefore, the PPAR α /p38/ROS/Akt axis may function as a central gatekeeper for platelet activation and is employed by major platelet receptors, such as immunoreceptor tyrosine-based activation motif receptor, G-protein-coupled receptors, and possibly CD36.

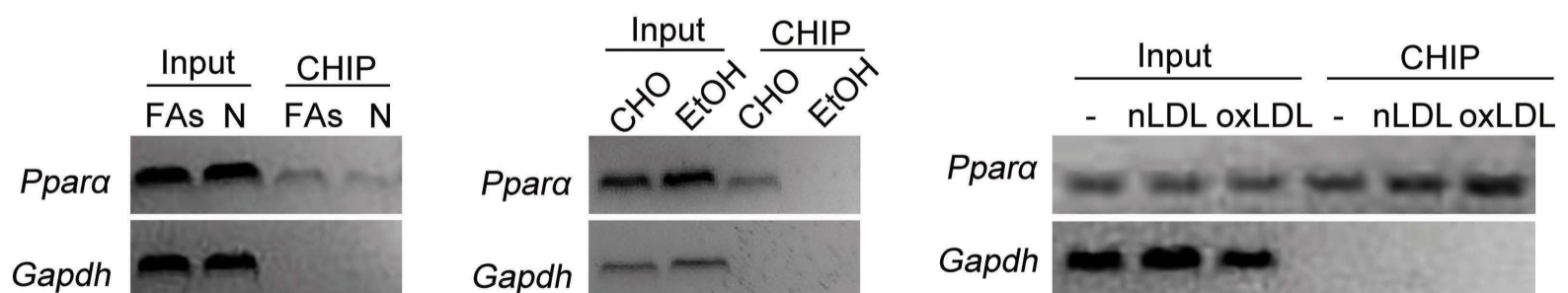
A key finding of the present study is the correlation between the level of expression of PPAR α and the extent of platelet reactivity. The subsequent data from the hyperlipidemic *Ppar α* ^{-/-}/*Apoe*^{-/-} mice model further revealed a causative relationship between PPAR α and platelet hyperactivity under the condition of hyperlipidemia. The correlation is found in both humans and mice, which indicates that it might be an evolutionary conservative mechanism. Unlike in macrophages, where oxLDL elevates the expression of both PPAR α ²¹ and PPAR γ ,³⁹ megakaryocytes seems to respond to hyperlipidemia specifically with upregulated expression of PPAR α , but not of PPAR β or PPAR γ . Considering the importance of fatty acids in supporting both megakaryocyte maturation⁴⁰ and platelet production,⁴¹ and the central roles of PPAR α in fatty acid metabolism,^{17,42} it may not be surprising that megakaryocyte PPAR α is a sensitive and specific target regulated by hyperlipidemia. Although it is commonly accepted that nongenomic mechanisms direct PPAR family-mediated platelet function,^{13,18,43,44} our findings suggest that in the case of PPAR α , a genomic regulation in megakaryocytes and a nongenomic signaling role in platelets are concerted to underscore the platelet hyperreactivity under hyperlipidemia.



E

Region 1 TCTGAGCGTGGTTTCCAGAGAAG-----TGGCCAGGATACTCCCAAGAGA-----
Region 2
Region 3 CGCCCTGGCACCTCCCGCCACC-----GACCTTGGACGGTCCCTCCACC-----
Region 4

Ppara gene
Gene ID: 5465



Legend on following page.

Figure 6. Oxidized low-density lipoproteins and lipids upregulate megakaryocyte but not platelet PPAR α . (A) Immunoblot analysis of PPAR α , PPAR β and PPAR γ expression in Meg-01 cells cultured with fatty acids (oleic acid [OA], 400 μ M and palmitic acid [PA], 200 μ M), cholesterol (CHO, 2.5 μ g/mL, 5.0 μ g/mL, 7.5 μ g/mL) or oxidized low-density lipoproteins (oxLDL, 10 μ g/mL, 50 μ g/mL) for 24 h with PPAR α , PPAR β and PPAR γ antibodies. Representative immunoblots from at least three independent experiments. (B) *PPARA* mRNA expression in Meg-01 cells cultured with fatty acids (OA, 400 μ M and PA, 200 μ M), cholesterol (CHO, 2.5 μ g/mL, 5.0 μ g/mL, 7.5 μ g/mL) or oxLDL (10 μ g/mL, 50 μ g/mL) for 24 h was analyzed by quantitative real-time polymerase chain reaction. Statistical significance was evaluated with a two-tailed Mann-Whitney test (* P <0.05; ns: not significant). (C) Immunoblot analysis of PPAR α and phosphorylated I κ B α level in Meg-01 cells cultured with fatty acids (OA, 400 μ M and PA, 200 μ M), cholesterol (CHO, 2.5 μ g/mL, 5.0 μ g/mL, 7.5 μ g/mL) or oxLDL (10 μ g/mL, 50 μ g/mL) in the absence or presence of BAY11-7082 (10 μ M) for 24 h. Representative immunoblots from at least three independent experiments. (D) Immunoblot analysis of PPAR α and phosphorylated I κ B α level in Meg-01 cells cultured with fatty acids (OA, 400 μ M and PA, 200 μ M), CHO (2.5 μ g/mL, 5.0 μ g/mL, 7.5 μ g/mL) or oxLDL (10 μ g/mL, 50 μ g/mL) in the absence or presence of *N*-acetylcysteine (NAC, 1 mM) or DTT (1 mM) for 24 h. Representative immunoblots from at least three independent experiments. (E) NF- κ B binding to the *Ppara* promoter of Meg-01 cells as determined by chromatin immunoprecipitation. Schematic diagram showing the NF- κ B-binding site in the *Ppara* promoter (top panel). Amplification of the *Ppara* promoter region containing the NF- κ B-binding motif in Meg-01 cells cultured with fatty acids (OA, 400 μ M and PA, 200 μ M), CHO (2.5 μ g/mL, 5.0 μ g/mL, 7.5 μ g/mL) or oxLDL (10 μ g/mL, 50 μ g/mL) for 24 h. GAPDH was used as a control to show precipitation specificity (bottom panel). Results shown are representative of three or more separate experiments run on different days.

In the current study, NF- κ B, activated by ROS, was revealed as the possible mechanism of the upregulation of PPAR α in megakaryocytes by hyperlipidemia. Our data suggest that NF- κ B upregulates PPAR α expression possibly through direct binding to the *Ppara* promoter region in lipid-treated megakaryocytes. It is worth mentioning that hyperglycemia elicits a similar NF- κ B activation which subsequently upregulates the expression of P2Y₁₂, a key receptor in mediating platelet activation and thrombosis.⁴⁵ It is therefore possible that metabolic disorders activate common inflammatory pathways to promote thrombosis. Interestingly, it was reported that PPAR α acts as a feedback to negatively regulate NF- κ B activation in smooth muscle cells⁴⁶ and the metabolism of the arachidonic acid metabolite leukotriene B₄ in hepatocytes.⁴⁷ It is yet to be determined whether PPAR α acts similarly in megakaryocytes to negatively regulate inflammation. However, while upregulation of PPAR α may suppress inflammation, it may exert a prothrombotic effect through enhanced platelet activation. PPAR α may thus be a key molecule maintaining the balance of thrombosis and inflammation, as suggested by the thrombo-inflammatory model of deep vein thrombosis in the current study.

The study has several limitations. First, expression of PPAR α in vascular cells has been reported;⁴⁸⁻⁵⁰ in the absence of a cell-specific knockout model, a possible contribution to hemostasis from vasculature PPAR α could not be excluded. Second, functional validation of the signaling involved was performed with inhibitors, which inevitably have possible off-target effects. Although it is beyond the scope of the study to chase every off-target effect, care must be taken when interpreting the results.

To summarize, we found that platelet PPAR α positively

mediates platelet activation through promoting dense granule secretion. Hyperlipidemia may contribute to the prothrombotic status through upregulated expression of PPAR α in megakaryocytes/platelets and enhanced activation signaling mediated by PPAR α in platelets. This work suggested that coupled genomic and nongenomic interventions targeting PPAR α may be necessary for the prevention of thrombosis under hyperlipidemia.

Disclosures

No conflicts of interest to disclose.

Contributions

LL, JZ and SW performed experiments, analyzed data, and wrote and revised the manuscript. LJ, XC and YZ performed experiments, analyzed data, and revised the manuscript. JL, JS, PL, ZS and FJG contributed intellectually and revised the manuscript. AL and HH designed the study and revised the manuscript.

Acknowledgments

The authors would like to thank the core facilities and the Center of Cryo-Electron Microscopy of Zhejiang University School of Medicine for technical support. The authors would also like to thank Ms. Xueping Zhou for excellent assistance in animal facilities.

Funding

This study was supported by grants from the National Natural Science Foundation of China (81870106, 82070138 to HH and 82000139 to PL) and the Zhejiang Provincial Natural Science Foundation (LZ18H080001 to HH and LQ21H030003 to ZS).

References

- Skulas-Ray AC, Wilson PWF, Harris WS, et al. Omega-3 fatty acids for the management of hypertriglyceridemia: a science advisory from the American Heart Association. *Circulation*. 2019;140(12):e673-e691.

2. Korporaal SJ, Meurs I, Hauer AD, et al. Deletion of the high-density lipoprotein receptor scavenger receptor BI in mice modulates thrombosis susceptibility and indirectly affects platelet function by elevation of plasma free cholesterol. *Arterioscler Thromb Vasc Biol.* 2011;31(1):34-42.
3. Maschberger P, Bauer M, Baumann-Siemons J, et al. Mildly oxidized low density lipoprotein rapidly stimulates via activation of the lysophosphatidic acid receptor Src family and Syk tyrosine kinases and Ca²⁺ influx in human platelets. *J Biol Chem.* 2000;275(25):19159-19166.
4. Cipollone F, Mezzetti A, Porreca E, et al. Association between enhanced soluble CD40L and prothrombotic state in hypercholesterolemia: effects of statin therapy. *Circulation.* 2002;106(4):399-402.
5. Korporaal SJ, Gorter G, van Rijn HJ, Akkerman JW. Effect of oxidation on the platelet-activating properties of low-density lipoprotein. *Arterioscler Thromb Vasc Biol.* 2005;25(4):867-872.
6. Wraith KS, Magwenzi S, Aburima A, Wen Y, Leake D, Naseem KM. Oxidized low-density lipoproteins induce rapid platelet activation and shape change through tyrosine kinase and Rho kinase-signaling pathways. *Blood.* 2013;122(4):580-589.
7. Chen K, Febbraio M, Li W, Silverstein RL. A specific CD36-dependent signaling pathway is required for platelet activation by oxidized low-density lipoprotein. *Circ Res.* 2008;102(12):1512-1519.
8. Yang M, Cooley BC, Li W, et al. Platelet CD36 promotes thrombosis by activating redox sensor ERK5 in hyperlipidemic conditions. *Blood.* 2017;129(21):2917-2927.
9. Magwenzi S, Woodward C, Wraith KS, et al. Oxidized LDL activates blood platelets through CD36/NOX2-mediated inhibition of the cGMP/protein kinase G signaling cascade. *Blood.* 2015;125(17):2693-2703.
10. Moraes LA, Unsworth AJ, Vaiyapuri S, et al. Farnesoid X receptor and its ligands inhibit the function of platelets. *Arterioscler Thromb Vasc Biol.* 2016;36(12):2324-2333.
11. Unsworth AJ, Bye AP, Tannetta DS, et al. Farnesoid X receptor and liver X receptor ligands initiate formation of coated platelets. *Arterioscler Thromb Vasc Biol.* 2017;37(8):1482-1493.
12. Hashizume S, Akaike M, Azuma H, et al. Activation of peroxisome proliferator-activated receptor alpha in megakaryocytes reduces platelet-derived growth factor-BB in platelets. *J Atheroscler Thromb.* 2011;18(2):138-147.
13. Akbiyik F, Ray DM, Gettings KF, Blumberg N, Francis CW, Phipps RP. Human bone marrow megakaryocytes and platelets express PPARgamma, and PPARgamma agonists blunt platelet release of CD40 ligand and thromboxanes. *Blood.* 2004;104(5):1361-1368.
14. Ali FY, Davidson SJ, Moraes LA, et al. Role of nuclear receptor signaling in platelets: antithrombotic effects of PPARbeta. *FASEB J.* 2006;20(2):326-328.
15. Gilde AJ, van der Lee KA, Willemsen PH, et al. Peroxisome proliferator-activated receptor (PPAR) alpha and PPARbeta/delta, but not PPARgamma, modulate the expression of genes involved in cardiac lipid metabolism. *Circ Res.* 2003;92(5):518-524.
16. Lalloyer F, Wouters K, Baron M, et al. Peroxisome proliferator-activated receptor-alpha gene level differently affects lipid metabolism and inflammation in apolipoprotein E2 knock-in mice. *Arterioscler Thromb Vasc Biol.* 2011;31(7):1573-1579.
17. Badman MK, Pissios P, Kennedy AR, Koukos G, Flier JS, Maratos-Flier E. Hepatic fibroblast growth factor 21 is regulated by PPARalpha and is a key mediator of hepatic lipid metabolism in ketotic states. *Cell Metab.* 2007;5(6):426-437.
18. Ali FY, Armstrong PC, Dhanji AR, et al. Antiplatelet actions of statins and fibrates are mediated by PPARs. *Arterioscler Thromb Vasc Biol.* 2009;29(5):706-711.
19. Yeung J, Adili R, Yamaguchi A, et al. Omega-6 DPA and its 12-lipoxygenase-oxidized lipids regulate platelet reactivity in a nongenomic PPARalpha-dependent manner. *Blood Adv.* 2020;4(18):4522-4537.
20. Drosatos K, Pollak NM, Pol CJ, et al. Cardiac myocyte KLF5 regulates Ppara expression and cardiac function. *Circ Res.* 2016;118(2):241-253.
21. Yu X, Li X, Zhao G, et al. OxLDL up-regulates Niemann-Pick type C1 expression through ERK1/2/COX-2/PPARalpha-signaling pathway in macrophages. *Acta Biochim Biophys Sin (Shanghai).* 2012;44(2):119-128.
22. Sartippour MR, Renier G. Differential regulation of macrophage peroxisome proliferator-activated receptor expression by glucose : role of peroxisome proliferator-activated receptors in lipoprotein lipase gene expression. *Arterioscler Thromb Vasc Biol.* 2000;20(1):104-110.
23. Lee SS, Pineau T, Drago J, et al. Targeted disruption of the alpha isoform of the peroxisome proliferator-activated receptor gene in mice results in abolishment of the pleiotropic effects of peroxisome proliferators. *Mol Cell Biol.* 1995;15(6):3012-3022.
24. Jiang L, Xu C, Yu S, et al. A critical role of thrombin/PAR-1 in ADP-induced platelet secretion and the second wave of aggregation. *J Thromb Haemost.* 2013;11(5):930-940.
25. Shi P, Zhang L, Zhang M, et al. Platelet-specific p38alpha deficiency improved cardiac function after myocardial infarction in mice. *Arterioscler Thromb Vasc Biol.* 2017;37(12):e185-e196.
26. Arthur JF, Qiao J, Shen Y, et al. ITAM receptor-mediated generation of reactive oxygen species in human platelets occurs via Syk-dependent and Syk-independent pathways. *J Thromb Haemost.* 2012;10(6):1133-1141.
27. Lu Y, Harada M, Kamijo Y, et al. Peroxisome proliferator-activated receptor alpha attenuates high-cholesterol diet-induced toxicity and pro-thrombotic effects in mice. *Arch Toxicol.* 2019;93(1):149-161.
28. Cominacini L, Pasini AF, Garbin U, et al. Oxidized low density lipoprotein (ox-LDL) binding to ox-LDL receptor-1 in endothelial cells induces the activation of NF-kappaB through an increased production of intracellular reactive oxygen species. *J Biol Chem.* 2000;275(17):12633-12638.
29. Zhuang P, Zhang Y, He W, et al. Dietary fats in relation to total and cause-specific mortality in a prospective cohort of 521 120 individuals with 16 years of follow-up. *Circ Res.* 2019;124(5):757-768.
30. Roy A, Jana M, Kundu M, et al. HMG-CoA reductase inhibitors bind to PPARalpha to upregulate neurotrophin expression in the brain and improve memory in mice. *Cell Metab.* 2015;22(2):253-265.
31. Xu HE, Stanley TB, Montana VG, et al. Structural basis for antagonist-mediated recruitment of nuclear co-repressors by PPARalpha. *Nature.* 2002;415(6873):813-817.
32. Stojanovic A, Marjanovic JA, Brovkovich VM, et al. A phosphoinositide 3-kinase-AKT-nitric oxide-cGMP signaling pathway in stimulating platelet secretion and aggregation. *J Biol Chem.* 2006;281(24):16333-16339.
33. O'Brien KA, Stojanovic-Terpo A, Hay N, Du X. An important role for Akt3 in platelet activation and thrombosis. *Blood.* 2011;118(15):4215-4223.
34. Kamiyama M, Shirai T, Tamura S, et al. ASK1 facilitates tumor metastasis through phosphorylation of an ADP receptor P2Y12 in platelets. *Cell Death Differ.* 2017;24(12):2066-2076.
35. Teissier E, Nohara A, Chinetti G, et al. Peroxisome proliferator-activated receptor alpha induces NADPH oxidase activity in macrophages, leading to the generation of LDL with PPAR-alpha

- activation properties. *Circ Res.* 2004;95(12):1174-1182.
36. Choo HJ, Saafir TB, Mkumba L, Wagner MB, Jobe SM. Mitochondrial calcium and reactive oxygen species regulate agonist-initiated platelet phosphatidylserine exposure. *Arterioscler Thromb Vasc Biol.* 2012;32(12):2946-2955.
37. Bakdash N, Williams MS. Spatially distinct production of reactive oxygen species regulates platelet activation. *Free Radic Biol Med.* 2008;45(2):158-166.
38. Liu Y, Hu M, Luo D, et al. Class III PI3K positively regulates platelet activation and thrombosis via PI(3)P-directed function of NADPH oxidase. *Arterioscler Thromb Vasc Biol.* 2017;37(11):2075-2086.
39. Ricote M, Huang J, Fajas L, et al. Expression of the peroxisome proliferator-activated receptor gamma (PPARgamma) in human atherosclerosis and regulation in macrophages by colony stimulating factors and oxidized low density lipoprotein. *Proc Natl Acad Sci U S A.* 1998;95(13):7614-7619.
40. Valet C, Batut A, Vauclard A, et al. Adipocyte fatty acid transfer supports megakaryocyte maturation. *Cell Rep.* 2020;32(1):107875.
41. Kelly KL, Reagan WJ, Sonnenberg GE, et al. De novo lipogenesis is essential for platelet production in humans. *Nat Metab.* 2020;2(10):1163-1178.
42. Ide T, Shimano H, Yoshikawa T, et al. Cross-talk between peroxisome proliferator-activated receptor (PPAR) alpha and liver X receptor (LXR) in nutritional regulation of fatty acid metabolism. II. LXRs suppress lipid degradation gene promoters through inhibition of PPAR signaling. *Mol Endocrinol.* 2003;17(7):1255-1267.
43. Moraes LA, Spyridon M, Kaiser WJ, et al. Non-genomic effects of PPARgamma ligands: inhibition of GPVI-stimulated platelet activation. *J Thromb Haemost.* 2010;8(3):577-587.
44. Ali FY, Hall MG, Desvergne B, Warner TD, Mitchell JA. PPARbeta/delta agonists modulate platelet function via a mechanism involving PPAR receptors and specific association/repression of PKCalpha--brief report. *Arterioscler Thromb Vasc Biol.* 2009;29(11):1871-1873.
45. Hu L, Chang L, Zhang Y, et al. Platelets express activated P2Y12 receptor in patients with diabetes mellitus. *Circulation.* 2017;136(9):817-833.
46. Delerive P, De Bosscher K, Besnard S, et al. Peroxisome proliferator-activated receptor alpha negatively regulates the vascular inflammatory gene response by negative cross-talk with transcription factors NF-kappaB and AP-1. *J Biol Chem.* 1999;274(45):32048-32054.
47. Devchand PR, Keller H, Peters JM, Vazquez M, Gonzalez FJ, Wahli W. The PPARalpha-leukotriene B4 pathway to inflammation control. *Nature.* 1996;384(6604):39-43.
48. Staels B, Koenig W, Habib A, et al. Activation of human aortic smooth-muscle cells is inhibited by PPARalpha but not by PPARgamma activators. *Nature.* 1998;393(6687):790-793.
49. Inoue I, Shino K, Noji S, Awata T, Katayama S. Expression of peroxisome proliferator-activated receptor alpha (PPAR alpha) in primary cultures of human vascular endothelial cells. *Biochem Biophys Res Commun.* 1998;246(2):370-374.
50. Chinetti G, Gbaguidi FG, Griglio S, et al. CLA-1/SR-BI is expressed in atherosclerotic lesion macrophages and regulated by activators of peroxisome proliferator-activated receptors. *Circulation.* 2000;101(20):2411-2417.